# Multiple Self-Trapped Emissions in the Lead-Free Halide $Cs_3 Cu_2I_5$

Chen, Haijie; Pina, Joao M.; Yuan, Fanglong; Johnston, Andrew; Ma, Dongxin; Chen, Bin; Li, Ziliang; Dumont, Antoine; Li, Xiyan; Liu, Yanan; Hoogland, Sjoerd; Zajacz, Zoltan; Lu, Zhenghong; Sargent, Edward H.

**How to cite**

CHEN, Haijie et al. Multiple Self-Trapped Emissions in the Lead-Free Halide $Cs_3 Cu_2I_5$. In: The journal of physical chemistry letters, 2020, vol. 11, p. 4326–4330. doi: 10.1021/acs.jpclett.0c01166

This publication URL: https://archive-ouverte.unige.ch/unige:163906
Publication DOI: 10.1021/acs.jpclett.0c01166

THE JOURNAL OF PHYSICAL CHEMISTRY Letters

pubs.acs.org/JPCL Letter

# Multiple Self-Trapped Emissions in the Lead-Free Halide $Cs_3Cu_2I_5$

Haijie Chen, Joao M. Pina, Fanglong Yuan, Andrew Johnston, Dongxin Ma, Bin Chen, Ziliang Li, Antoine Dumont, Xiyan Li, Yanan Liu, Sjoerd Hoogland, Zoltán Zajacz, Zhenghong Lu, and Edward H. Sargent*

Cite This: J. Phys. Chem. Lett. 2020, 11, 4326–4330 Read Online

ACCESS | Metrics & More | Article Recommendations | Supporting Information

**ABSTRACT:** Low-dimensional copper halides with high luminance have attracted increasing interest as heavy-metal-free light emitters. However, the optical mechanisms underpinning their excellent luminescence remain underexplored. Here, we report multiple self-trapped emissions in $Cs_3Cu_2I_5$. Power-dependent photoluminescence spectra reveal the appearance of multiple self-trapped emission peaks with increasing excitation power, and this emission behavior is explored across a temperature range of 80−420 K. The zero-dimensional structure and soft crystal lattice contribute to the multiple self-trapped emissions in $Cs_3Cu_2I_5$: this explains the origin of the broad emission and the luminescence mechanism in $Cs_3Cu_2I_5$ and will assist in improving our understanding of the optical properties of other metal halides. We incorporate the $Cs_3Cu_2I_5$ in light-emitting diodes that achieve a peak luminance of 140 cd/m$^2$ and an external quantum efficiency of 0.27%.

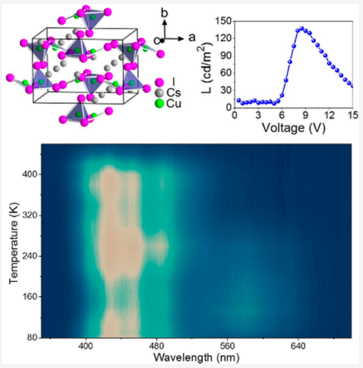




Lead halide perovskites have advanced rapidly as light-emitting materials in view of their narrow emission line width, defect tolerance, and simple processing.[1,2] Finding routes that avoid the use of lead in light-emitting diodes (LEDs) remains of interest.[3,4] The ready oxidation of $Sn^{2+}$ to $Sn^{4+}$ motivates continued work in other metal selections, as do the limitations on the efficiency and conductivity in Ge-, Bi-, and Sb-based halides.[5−7]

Blue-emitting $Cs_3Cu_2I_5$ has recently shown impressive progress.[8,9] A near-unity photoluminescence quantum yield (PLQY) was also observed in the Br analogue.[10] In $CsCu_2I_3$, white-light emission was observed in single crystals,[11] while yellow luminescence was obtained in nanocrystals.[12] Interestingly, strong blue emission was also observed in the new compounds $Rb_8CuSc_3Cl_{18}$ and $Rb_8CuY_3Cl_{18}$, indicating that Cu plays an important role in the photoluminescence mechanism.[13]

Here we investigate the photoluminescence (PL) mechanism of $Cs_3Cu_2I_5$ and explore the use of this material in LEDs. On the basis of the power- and temperature-dependent PL spectra, we find that the broad photoluminescence centered at 436 nm arises due to distinct self-trapped emission peaks, a fact that we attribute to the zero-dimensional (0D) structure and soft crystal lattice. By tailoring the synthesis conditions of $Cs_3Cu_2I_5$, we achieve a record-high PLQY of near unity in as-prepared thin films. Using NFI-modified PEDOT:PSS as the hole transport layer (HTL) and poly-HEMA as the additive in the emitting layer, we develop blue LEDs with a peak external quantum efficiency (EQE) of ∼0.27% and a maximum luminance of 140 cd/m$^2$.

Two known Cs−Cu−I compounds exist: $Cs_3Cu_2I_5$ and $CsCu_2I_3$ (crystal structures in Figure 1).[14,15] $Cs_3Cu_2I_5$ adopts a

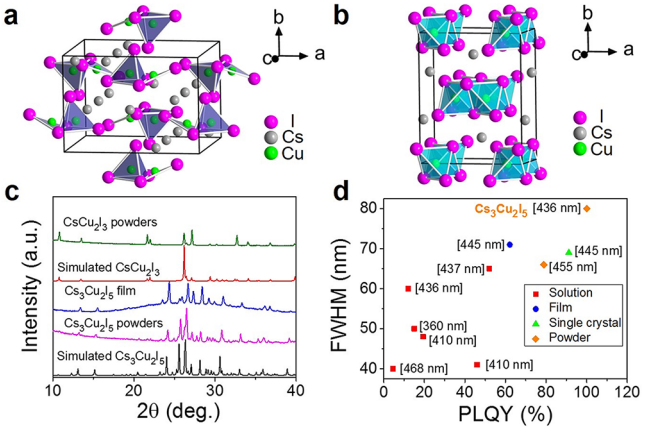


**Figure 1.** Crystal structures of (a) $Cs_3Cu_2I_5$ and (b) $CsCu_2I_3$. (c) X-ray diffraction of the as-synthesized $CsCu_2I_3$ and $Cs_3Cu_2I_5$ powders and $Cs_3Cu_2I_5$ film, compared with the corresponding simulated patterns. (d) Performance table of blue-emitting lead-free halide materials.

Received: April 15, 2020
Accepted: May 11, 2020
Published: May 11, 2020




https://dx.doi.org/10.1021/acs.jpclett.0c01166
J. Phys. Chem. Lett. 2020, 11, 4326–4330

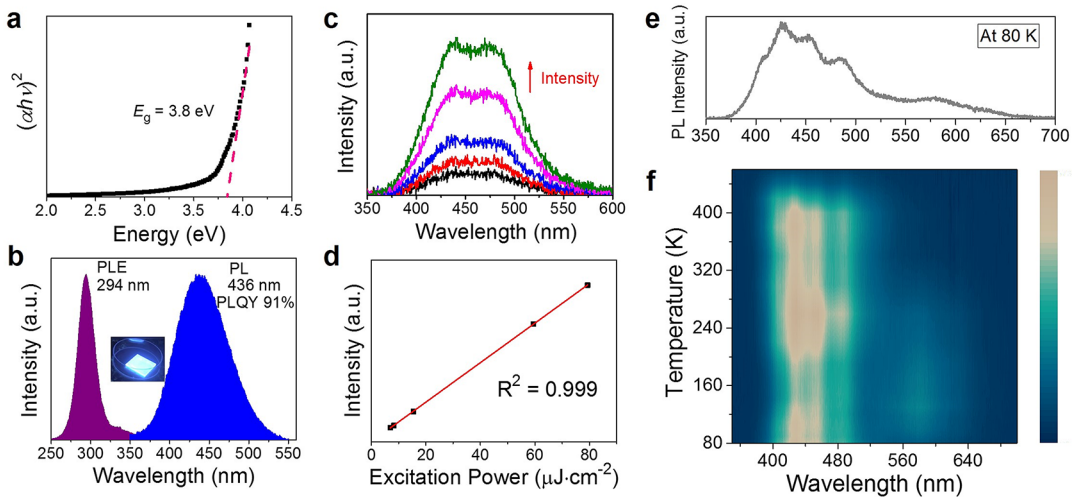


**Figure 2.** (a) Absorption spectrum of the $Cs_3Cu_2I_5$ film, indicating a band gap of 3.8 eV. (b) Photoluminescence excitation (PLE) and photoluminescence (PL) spectra of the $Cs_3Cu_2I_5$ thin film using a xenon lamp as the excitation source. The inset shows a photo of the as-synthesized film with shiny blue light under 265 nm light. (c) Power-dependent PL (250 fs, 5000 Hz excitation; fluence of <1 $\mu$J cm$^{-2}$) showing the appearance of multiple emission peaks while the excitation fluence is increasing. (d) Integrated PL intensity as a function of excitation power. (e and f) Temperature-dependent PL (at around 60 $\mu$J cm$^{-2}$ excitation) showing the appearance of multiple emission peaks at lower temperatures.

0D structure composed of $Cs^+$ ions and isolated $[Cu_2I_5]^{3-}$ fragments. As shown in Figure 1a, Cu atoms have two types of coordination: trigonal, surrounded by three I atoms, and tetrahedral, surrounded by four I atoms. For $CsCu_2I_3$, Cu is coordinated with four I atoms (Figure 1b). It crystallizes in a one-dimensional (1D) structure with double edge-shared $[CuI_4]^{3-}$ chains along the *c* axis. The structural difference leads to different optoelectrical properties in $Cs_3Cu_2I_5$ and $CsCu_2I_3$.

To study the Cs−Cu−I system, we synthesized the pure $Cs_3Cu_2I_5$ and $CsCu_2I_3$ phases. $CsCu_2I_3$ was obtained by VSA crystallization from a 1 M precursor solution (stoichiometric CsI and CuI) in a DMF/DMSO (50:50) solvent.[8] We were unable to synthesize $Cs_3Cu_2I_5$ single crystals using this method.

We instead employed a solid-state reaction with stoichiometric CsI and CuI (1:2 for $CsCu_2I_3$ and 3:2 for $Cs_3Cu_2I_5$) at 400 °C.[10] Powder X-ray diffraction (XRD) was used to characterize the as-synthesized materials (Figure 1c). $Cs_3Cu_2I_5$ and $CsCu_2I_3$ were found to be pure and single-phase. The PL spectra of these samples showed strong blue emission from $Cs_3Cu_2I_5$ and weak white emission for $CsCu_2I_3$, which is consistent with prior results.[9]

Both $Cs_3Cu_2I_5$ and $CsCu_2I_3$ were found to be stable in air. $Cs_3Cu_2I_5$ powders show a unity (100%) PLQY. Figure 1d shows the PL performance compared to that of the known blue-emitting lead-free halide materials.[16−21] $Cs_3Cu_2I_5$ is a more efficient emitter but has a broader emission spectrum. For the $Cs_3Cu_2I_5$ thin film, there is no diffraction signal (Figure 1c) from $CsCu_2I_3$, indicating purity of phase.

We obtained a band gap of 3.8 eV for $Cs_3Cu_2I_5$ from the UV−vis absorption spectrum (Figure 2a), which is consistent with previous reports.[8] A second, lower-energy, absorption feature at ∼3.6 eV is also observed, which suggests another transition that is yet to be reported. The photoluminescence excitation (PLE) and PL spectra of the $Cs_3Cu_2I_5$ thin film are shown in Figure 2b. The PLE spectra show a second absorption feature in the form of a red-shifted tail (in the range of 3.6−3.8 eV) from the main PLE peak, consistent with the lower-energy absorption feature shown in Figure 2a. Other features in the PLE spectra are further distinguished through the second derivatives of the spectra (Figure S1a).[8] At low excitation fluences, the blue PL is centered at 436 nm with a high PLQY of 91%. A small asymmetry is detected in the PL spectra of Figure 2b, which is better fit using an exponentially modified Gaussian than by a single Gaussian distribution (Figure S1b), suggesting an overlapped emission of the main emission peak with lower-intensity transitions. This multi-transition radiative behavior is accentuated with increasing excitation fluence, as shown in Figure 2c and Figure S2, where a clear second emission peak is present. The high PLQY is maintained even at high excitation fluences, as shown by the linear increase in radiative intensity with excitation power shown in Figure 2d. Temperature-dependent studies at high fluences show the appearance of other emission peaks that can be attributed to structured emission due to strong exciton coupling to lattice vibrations.

Previous reports about the PL mechanism of $Cs_3Cu_2I_5$ differ. Some have proposed energy transfer as a result of the structural distortion, while others offer self-trapped excitons as a possible explanation.[10] The explanation of self-trapped excitons is consistent with the large Stokes shift in $Cs_3Cu_2I_5$. The similar emission wavelengths of $Cs_3Cu_2Br_5$ and $Cs_3Cu_2I_5$ (455 and 443 nm, respectively) indicate that the emission mechanism in these compound originates from the copper halide clusters contained in the structure.[10] As such, it is also natural to consider the emission mechanisms in CuI crystals, where multiemission peaks have been reported and attributed to defect-induced emission.[22,23] However, defect-induced emission often leads to fast intensity saturation,[10,24,25] a trend different from that seen in Figure 2d. The multipeak emission with a large Stokes shift is also present at low temperatures (Figure 2e), which argues against a defect-based emission mechanism. It has been previously reported that carriers are frozen at low temperatures, leading to improved band-to-band radiative emission due to the decreased efficiency to reach trap centers. No signal of band-to-band emission is obtained at cryogenic temperatures. Furthermore, the PLE spectra (Figure 2b) did not show a subgap contribution (located near the emission center) to the PL, something that is normally seen


https://dx.doi.org/10.1021/acs.jpclett.0c01166
J. Phys. Chem. Lett. 2020, 11, 4326−4330

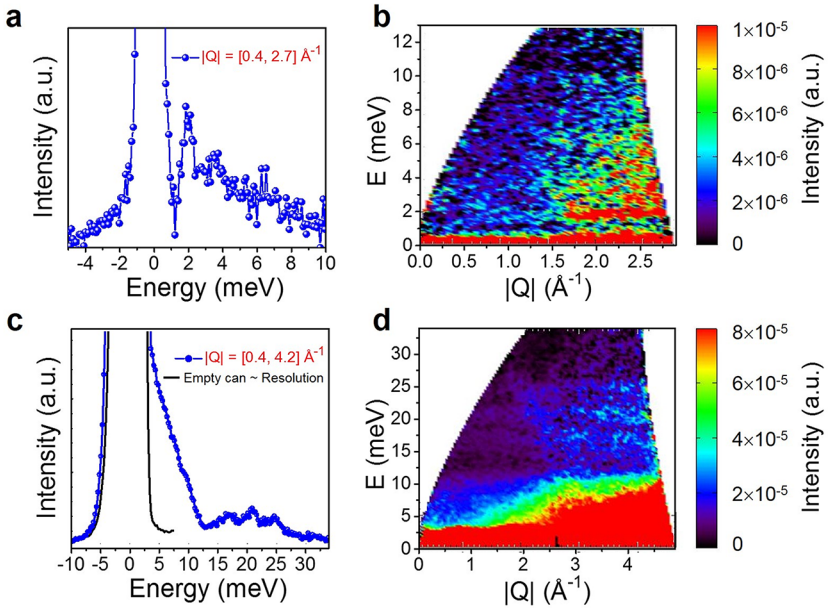


**Figure 3.** Dynamical structure factor $S(Q, E)$ of $Cs_3Cu_2I_5$ integrated over momentum transfer $Q$ (a and c) and contour plots of $S(Q, E)$ (b and d), obtained from INS spectra measured with $E_i$ values of 18 meV (a and b) and 55 meV (c and d).

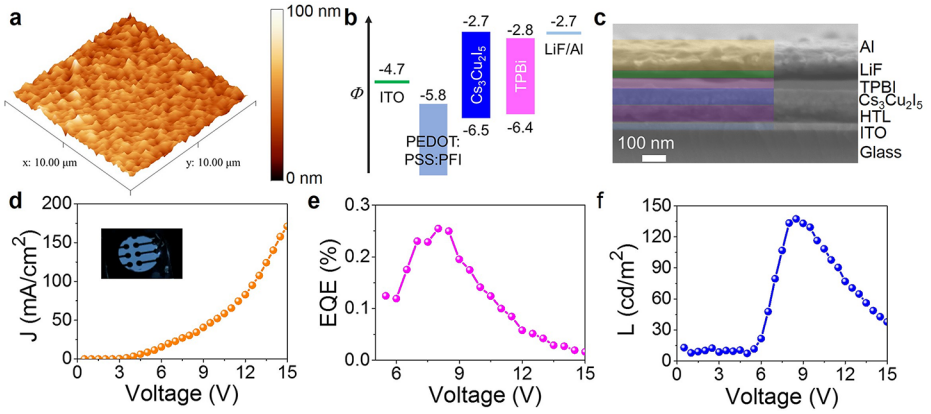


**Figure 4.** (a) AFM picture of the as-synthesized $Cs_3Cu_2I_5$ film. (b) Energy band alignment of the LED device. (c) Cross-sectional SEM image of the LED device (artificially colored). (d) Current density ($J$), (e) external quantum efficiency (EQE), and (f) luminance ($L$) vs applied voltage characteristics of the device with a $Cs_3Cu_2I_5$-poly-HEMA emission layer. A photo of the blue-emitting device is the inset in panel d.

with permanent defects. These results agree with the view that defect-based emission is not the dominant emission mechanism. It is noted that the range of fluence used in Figure 2d is limited (roughly ranging from 7 to 80 $\mu$J cm$^{-2}$, 1 order of magnitude, while presumably characterization in a lower and higher excitation fluence regime would be desirable). Ideally, we would characterize the material until it reaches saturation. The absorption edge of the material is ~3.8 eV (around 330 nm), and the 315 nm source available to us was limited in its dynamic range. A wider range of fluences and the PL decay kinetics at different excitation pulse densities would be desirable in future studies.

In Figure 2f, we show that additional emission exists at ~550 nm at temperatures below 280 K. Emissive transitions from copper halide clusters are due to Cu 3d to Cu 4s transitions. In the ground state, Cu(I)-d$^{10}$ complexes are known to favor a tetrahedral geometry that is transformed into a tetragonally flattened structure upon excitation to form Cu(II)-d$^9$.[26] A recent report about the 1D copper halides suggests the existence of multiple emissions by first-principles calculation.[27] They suggest that the multiple emission peaks are due to low-dimensional copper halide clusters and the soft crystal lattice. In $Cs_3Cu_2I_5$, the Jahn−Teller distorted Cu(II)-d$^9$ center arises due to the otherwise unequal occupation of the degenerate t2 3d orbitals and may explain the observed Stokes shift and multiple emissions. There has been no report about the absorption cross section of $Cs_3Cu_2I_5$ until now, and the accurate carrier concentration in the film is unknown. Referring to the commonly reported halides, we coarsely estimate a carrier density on the order of ~$10^{16}$−$10^{17}$ cm$^{-3}$ in our film.

To evaluate the crystal lattice rigidity, we measured the dynamical structure factor of $S(Q, E)$, which is proportional to the generalized phonon density of states, of the as-synthesized $Cs_3Cu_2I_5$ thin film. The contour plot of $S(Q, E)$ and that integrated over momentum transfer intensities for the spectra measured with $E_i$ values of 18 and 50 meV are shown in Figure 3. The phonon spectrum of the $Cs_3Cu_2I_5$ thin film extends to ~30 meV [with three optical peaks at ~17, ~21, and ~25 meV (Figure 3d)] and has a strong increase of intensity at energies


https://dx.doi.org/10.1021/acs.jpclett.0c01166
J. Phys. Chem. Lett. 2020, 11, 4326−4330

below 10 meV (which is unresolved for the INS spectra for an $E_i$ of 50 meV). The high-resolution data obtained with an $E_i$ of 18 meV (Figure 3a) show two peaks in the range of acoustic phonons, at ∼2 meV (strong) and ∼3.5 meV. The observed soft mode demonstrates that $Cs_3Cu_2I_5$ has a soft lattice. This finding is consistent with multiple self-trapped emissions due to the 0D structure and ultrasoft crystal lattice.[27]

Encouraged by the high PLQY of films of $Cs_3Cu_2I_5$, we fabricated LEDs using $Cs_3Cu_2I_5$ films. Atomic force microscopy (AFM) was used to characterize the surface of the synthesized films. The results (Figure 4a) indicate a roughness of ∼10 nm. The film, smooth enough to avoid current leakage, is suitable for LED fabrication. Previous reports found that inverted LEDs do not work well for this material.[8]

We therefore used PEDOT:PSS as the hole injection layer (HIL). As shown in Figure 4b, the PEDOT:PSS was further doped with PFI for suitable band alignment.[28] Figure 4c shows the cross-sectional SEM image of the as-synthesized device. The different layers were marked with different colors. The architecture is ITO/PEDOT:PSS:PFI (60 nm)/$Cs_3Cu_2I_5$-poly-HEMA film (90 nm)/TPBI (50 nm)/LiF (1 nm)/Al (120 nm).

The emitting $Cs_3Cu_2I_5$ was mixed with the polymer poly-HEMA to form a heterostructure.[29] The emitting $Cs_3Cu_2I_5$-poly-HEMA layer forms a circular column-shaped film with a thickness of ∼90 nm. The measured voltage-dependent current density shows an increasing curve with an increase in voltage (Figure 4d). The maximal current is ∼180 mA/cm$^2$ at 15 V, indicating acceptable carrier injection and contact among layers. In Figure 4e, the maximal EQE is around 0.27%. The maximum luminance is 140 cd/m$^2$ (Figure 4f). It is found that the utilization of the poly-HEMA greatly improves the performance of the fabricated LED devices. As shown in Figure S3, the device without poly-HEMA gives a much poorer performance (maximal EQE of 0.07% and maximal luminance of 27 cd/m$^2$) than that with poly-HEMA. The formation of the $Cs_3Cu_2I_5$-poly-HEMA heterostructure enhances carrier injection. Compared to the reported LED performances based on lead-free halides, $Cs_3Cu_2I_5$ displays the highest luminance at the highest EQE value (Figure S4).[30,31]

We report $Cs_3Cu_2I_5$ exhibits a blue emission with a PLQY of 100%. We found that multiple self-trapped emission peaks emerge at increasing excitation powers and remain at low temperatures. This arises due to the 0D structure and ultrasoft crystal lattice of $Cs_3Cu_2I_5$, which were confirmed via measurement of the phonon intensity. The work suggests that the low-dimensional copper halides are promising nontoxic and stable materials with efficient special emissions. On the basis of the optimized band alignment between the HTL and the emitting layer, we demonstrated an LED device. We anticipate that Cu-based halides will provide a new direction for the exploration of lead-free materials for optoelectronic applications.

## ■ ASSOCIATED CONTENT

### Supporting Information

The Supporting Information is available free of charge at https://pubs.acs.org/doi/10.1021/acs.jpclett.0c01166.

Experimental section, second derivative of the photoluminescence excitation (PLE), fitting of the PL spectra, normalized multiple emission peaks at high and low excitation fluences, performance of the as-fabricated LED with only $Cs_3Cu_2I_5$ as the emission layer, and comparative performance of lead-free halide LEDs (PDF)

## ■ AUTHOR INFORMATION


### Corresponding Author

**Edward H. Sargent** − *The Edward S. Rogers Department of Electrical and Computer Engineering, University of Toronto, Toronto, Ontario, Canada M5S 3G4;* orcid.org/0000-0003-0396-6495; Email: ted.sargent@utoronto.ca

### Authors

**Haijie Chen** − *The Edward S. Rogers Department of Electrical and Computer Engineering, University of Toronto, Toronto, Ontario, Canada M5S 3G4;* orcid.org/0000-0003-3567-1763

**Joao M. Pina** − *The Edward S. Rogers Department of Electrical and Computer Engineering, University of Toronto, Toronto, Ontario, Canada M5S 3G4*

**Fanglong Yuan** − *The Edward S. Rogers Department of Electrical and Computer Engineering and Department of Materials Science and Engineering, University of Toronto, Toronto, Ontario, Canada M5S 3G4*

**Andrew Johnston** − *The Edward S. Rogers Department of Electrical and Computer Engineering, University of Toronto, Toronto, Ontario, Canada M5S 3G4;* orcid.org/0000-0002-4545-532X

**Dongxin Ma** − *The Edward S. Rogers Department of Electrical and Computer Engineering, University of Toronto, Toronto, Ontario, Canada M5S 3G4;* orcid.org/0000-0002-9790-5951

**Bin Chen** − *The Edward S. Rogers Department of Electrical and Computer Engineering, University of Toronto, Toronto, Ontario, Canada M5S 3G4*

**Ziliang Li** − *The Edward S. Rogers Department of Electrical and Computer Engineering, University of Toronto, Toronto, Ontario, Canada M5S 3G4*

**Antoine Dumont** − *Department of Materials Science and Engineering, University of Toronto, Toronto, Ontario, Canada M5S 3E4*

**Xiyan Li** − *The Edward S. Rogers Department of Electrical and Computer Engineering, University of Toronto, Toronto, Ontario, Canada M5S 3G4*

**Yanan Liu** − *Department of Earth Sciences, University of Toronto, Toronto, Ontario, Canada M5S 3B1*

**Sjoerd Hoogland** − *The Edward S. Rogers Department of Electrical and Computer Engineering, University of Toronto, Toronto, Ontario, Canada M5S 3G4*

**Zoltán Zajacz** − *Department of Earth Sciences, University of Toronto, Toronto, Ontario, Canada M5S 3B1*

**Zhenghong Lu** − *Department of Materials Science and Engineering, University of Toronto, Toronto, Ontario, Canada M5S 3E4;* orcid.org/0000-0003-2050-0822

Complete contact information is available at: https://pubs.acs.org/10.1021/acs.jpclett.0c01166


### Notes

The authors declare no competing financial interest.

## ■ ACKNOWLEDGMENTS

This work was financially supported by the Ontario Research Fund-Research Excellence Program and the Natural Sciences

and Engineering Research Council of Canada (NSERC) and by the Global Research Outreach program of the Samsung Advanced Institute of Technology. This research used resources at the Spallation Neutron Source, a U.S. Department of Energy Office of Science User Facility operated by the Oak Ridge National Laboratory. The authors thank Prof. Hideo Hosono and Prof. Junghwan Kim for useful discussions about the luminescence of these materials.

## REFERENCES

(1) Tan, Z.-K.; Moghaddam, R. S.; Lai, M. L.; Docampo, P.; Higler, R.; Deschler, F.; Price, M.; Sadhanala, A.; Pazos, L. M.; Credgington, D.; et al. Bright light-emitting diodes based on organometal halide perovskite. *Nat. Nanotechnol.* **2014**, *9* (9), 687−692.

(2) Lin, K.; Xing, J.; Quan, L. N.; de Arquer, F. P. G.; Gong, X.; Lu, J.; Xie, L.; Zhao, W.; Zhang, D.; Yan, C.; et al. Perovskite light-emitting diodes with external quantum efficiency exceeding 20%. *Nature* **2018**, *562* (7726), 245−248.

(3) Ke, W.; Stoumpos, C. C.; Kanatzidis, M. G. Unleaded" Perovskites: Status Quo and Future Prospects of Tin-Based Perovskite Solar Cells. *Adv. Mater.* **2019**, *31*, 1803230.

(4) Xiao, Z.; Song, Z.; Yan, Y. From Lead Halide Perovskites to Lead-Free Metal Halide Perovskites and Perovskite Derivatives. *Adv. Mater.* **2019**, *31*, 1803792.

(5) Stoumpos, C. C.; Frazer, L.; Clark, D. J.; Kim, Y. S.; Rhim, S. H.; Freeman, A. J.; Ketterson, J. B.; Jang, J. I.; Kanatzidis, M. G. Hybrid germanium iodide perovskite semiconductors: active lone pairs, structural distortions, direct and indirect energy gaps, and strong nonlinear optical properties. *J. Am. Chem. Soc.* **2015**, *137* (21), 6804−6819.

(6) Chang, J. H.; Doert, T.; Ruck, M. Structural Variety of Defect Perovskite Variants $M_3E_2X_9$ (M= Rb, Tl, E= Bi, Sb, X= Br, I). *Z. Anorg. Allg. Chem.* **2016**, *642* (13), 736−748.

(7) Luo, J.; Wang, X.; Li, S.; Liu, J.; Guo, Y.; Niu, G.; Yao, L.; Fu, Y.; Gao, L.; Dong, Q.; et al. Efficient and stable emission of warm-white light from lead-free halide double perovskites. *Nature* **2018**, *563* (7732), 541−545.

(8) Jun, T.; Sim, K.; Iimura, S.; Sasase, M.; Kamioka, H.; Kim, J.; Hosono, H. Lead-Free Highly Efficient Blue-Emitting $Cs_3Cu_2I_5$ with 0D Electronic Structure. *Adv. Mater.* **2018**, *30* (43), 1804547.

(9) Cheng, P.; Sun, L.; Feng, L.; Yang, S.; Yang, Y.; Zheng, D.; Zhao, Y.; Sang, Y.; Zhang, R.; Wei, D.; Deng, W.; Han, K. Colloidal Synthesis and Optical Properties of All-Inorganic Low-Dimensional Cesium Copper Halide Nanocrystals. *Angew. Chem.* **2019**, *131*, 16233−16237.

(10) Roccanova, R.; Yangui, A.; Nhalil, H.; Shi, H.; Du, M.-H.; Saparov, B. Near-Unity Photoluminescence Quantum Yield in Blue-Emitting $Cs_3Cu_2Br_{5-x}I_x$ ($0 \le x \le 5$). *ACS Appl. Electron. Mater.* **2019**, *1* (3), 269−274.

(11) Lin, R.; Guo, Q.; Zhu, Q.; Zhu, Y.; Zheng, W.; Huang, F. All-Inorganic $CsCu_2I_3$ Single Crystal with High-PLQY (≈ 15.7%) Intrinsic White-Light Emission via Strongly Localized 1D Excitonic Recombination. *Adv. Mater.* **2019**, *31*, 1905079.

(12) Vashishtha, P.; Nutan, G. V.; E. Griffith, B.; Fang, Y.; Giovanni, D.; Jagadeeswararao, M.; Sum, T. C.; Mathews, N.; Mhaisalkar, S. G.; Hanna, J. V.; White, T. Cesium Copper Iodide Tailored Nanoplates and Nanorods for Blue, Yellow, and White Emission. *Chem. Mater.* **2019**, *31* (21), 9003−9011.

(13) Lin, J.; Chen, H.; Kang, J.; Quan, L. N.; Lin, Z.; Kong, Q.; Lai, M.; Yu, S.; Wang, L.; Wang, L.-w.; Toney, M. F.; Yang, P. Copper (I)-Based Highly Emissive All-Inorganic Rare-Earth Halide Clusters. *Matter* **2019**, *1* (1), 180−191.

(14) Jouini, N.; Guen, L.; Tournoux, M. Crystal Structure of cesium copper iodide ($CsCu_2I_3$). *Rev. Chim. Miner.* **1981**, *17* (5), 486−491.

(15) Bigalke, K.; Hans, A.; Hartl, H. Synthese und Struktur-untersuchungen von Iodocupraten (I). IX. Synthese und Kristall-strukturen von $Cs_3Cu_2I_5$ und $RbCu_2I_3$. *Z. Anorg. Allg. Chem.* **1988**, *563* (1), 96−104.

(16) Leng, M.; Yang, Y.; Zeng, K.; Chen, Z.; Tan, Z.; Li, S.; Li, J.; Xu, B.; Li, D.; Hautzinger, M. P.; et al. All-inorganic bismuth-based perovskite quantum dots with bright blue photoluminescence and excellent stability. *Adv. Funct. Mater.* **2018**, *28* (1), 1704446.

(17) Leng, M.; Chen, Z.; Yang, Y.; Li, Z.; Zeng, K.; Li, K.; Niu, G.; He, Y.; Zhou, Q.; Tang, J. Lead-free, blue emitting bismuth halide perovskite quantum dots. *Angew. Chem., Int. Ed.* **2016**, *55* (48), 15012−15016.

(18) Zhang, J.; Yang, Y.; Deng, H.; Farooq, U.; Yang, X.; Khan, J.; Tang, J.; Song, H. High quantum yield blue emission from lead-free inorganic antimony halide perovskite colloidal quantum dots. *ACS Nano* **2017**, *11* (9), 9294−9302.

(19) Tan, Z.; Li, J.; Zhang, C.; Li, Z.; Hu, Q.; Xiao, Z.; Kamiya, T.; Hosono, H.; Niu, G.; Lifshitz, E.; Cheng, Y.; Tang, J. Highly Efficient Blue-Emitting Bi-Doped $Cs_2SnCl_6$ Perovskite Variant: Photoluminescence Induced by Impurity Doping. *Adv. Funct. Mater.* **2018**, *28* (29), 1801131.

(20) Yang, B.; Chen, J.; Hong, F.; Mao, X.; Zheng, K.; Yang, S.; Li, Y.; Pullerits, T.; Deng, W.; Han, K. Lead-free, air-stable all-inorganic cesium bismuth halide perovskite nanocrystals. *Angew. Chem., Int. Ed.* **2017**, *56* (41), 12471−12475.

(21) Shen, Y.; Yin, J.; Cai, B.; Wang, Z.; Dong, Y.; Xu, X.; Zeng, H. Lead-free, stable, high-efficiency (52%) blue luminescent $FA_3Bi_2Br_9$ perovskite quantum dots. *Nanoscale Horiz.* **2020**, *5*, 580−585.

(22) Chen, D.; Wang, Y.; Lin, Z.; Huang, J.; Chen, X.; Pan, D.; Huang, F. Growth strategy and physical properties of the high mobility p-type CuI crystal. *Cryst. Growth Des.* **2010**, *10* (5), 2057−2060.

(23) Gao, P.; Gu, M.; Liu, X.; Zheng, Y. Q.; Shi, E. W. Photoluminescence study of annealing effects on CuI crystals grown by evaporation method. *Cryst. Res. Technol.* **2012**, *47* (7), 707−712.

(24) Zhou, C.; Lin, H.; Tian, Y.; Yuan, Z.; Clark, R.; Chen, B.; van de Burgt, L. J.; Wang, J. C.; Zhou, Y.; Hanson, K.; et al. Luminescent zero-dimensional organic metal halide hybrids with near-unity quantum efficiency. *Chem. Sci.* **2018**, *9* (3), 586−593.

(25) Han, D.; Shi, H.; Ming, W.; Zhou, C.; Ma, B.; Saparov, B.; Ma, Y.-Z.; Chen, S.; Du, M.-H. Unraveling luminescence mechanisms in zero-dimensional halide perovskites. *J. Mater. Chem. C* **2018**, *6* (24), 6398−6405.

(26) Kim, Y.-E.; Kim, J.; Park, J. W.; Park, K.; Lee, Y. $\sigma$-Complexation as a strategy for designing copper-based light emitters. *Chem. Commun.* **2017**, *53* (19), 2858−2861.

(27) Du, M.-H. Emission Trend of Multiple Self-Trapped Excitons in Luminescent 1D Copper Halides. *ACS Energy Lett.* **2020**, *5* (2), 464−469.

(28) Vreeland, R. F.; Atcherley, C. W.; Russell, W. S.; Xie, J. Y.; Lu, D.; Laude, N. D.; Porreca, F.; Heien, M. L. Biocompatible PEDOT: Nafion composite electrode coatings for selective detection of neurotransmitters in vivo. *Anal. Chem.* **2015**, *87* (5), 2600−2607.

(29) Zhao, B.; Bai, S.; Kim, V.; Lamboll, R.; Shivanna, R.; Auras, F.; Richter, J. M.; Yang, L.; Dai, L.; Alsari, M.; et al. High-efficiency perovskite−polymer bulk heterostructure light-emitting diodes. *Nat. Photonics* **2018**, *12* (12), 783−789.

(30) Zhang, X.; Wang, C.; Zhang, Y.; Zhang, X.; Wang, S.; Lu, M.; Cui, H.; Kershaw, S. V.; Yu, W. W.; Rogach, A. L. Bright orange electroluminescence from lead-free two-dimensional perovskites. *ACS Energy Lett.* **2019**, *4* (1), 242−248.

(31) Ma, Z.; Shi, Z.; Yang, D.; Zhang, F.; Li, S.; Wang, L.; Wu, D.; Zhang, Y.; Na, G.; Zhang, L.; et al. Electrically-Driven Violet Light-Emitting Devices Based on Highly Stable Lead-Free Perovskite $Cs_3Sb_2Br_9$ Quantum Dots. *ACS Energy Lett.* **2020**, *5*, 385−394.



https://dx.doi.org/10.1021/acs.jpclett.0c01166
J. Phys. Chem. Lett. 2020, 11, 4326−4330